Improvement of the Inversion Procedure in Resonant Ultrasound Spectroscopy for Generally Oriented, High Anisotropic Crystals

Hanuš Seiner, Petr Sedlák
Faculty of Nuclear Sciences and Physical Engineering,
Czech Technical University in Prague,
Prague, the Czech Republic
E-mail: hseiner@it.cas.cz

Michal Landa
Institute of Thermomechanics,
Academy of Sciences of the Czech Republic,
Prague, the Czech Republic
E-mail: ml@it.cas.cz

***Abstract*—This paper presents an improvement of the resonant ultrasound spectroscopy (RUS) inverse procedure for determination of elastic properties of shape memory alloys. Reliable mode identification and, thus, a well-posed resonance inversion was achieved by evaluation of both resonance frequencies and eigenvibration modes using a scanning laser interferometry measurement. The proposed approach was verified on determination of elastic constants and their temperature dependences of austenitic and martensitic phases of CuAlNi single crystals. The results on CuAlNi well correspond to our previous obtained by the pulse-echo measurement. The method can be applied for twinned structures, which enables investigation of naturally twinned shape memory alloys.**

Keywords- resonant ulresound spectroscopy, inverse problem, shape memory alloys

I. INTRODUCTION

Resonant ultrasound spectroscopy (RUS) is a well-known technique for determination of elastic properties of solids based on measurements of natural frequencies of free elastic vibrations of a small, simply shaped specimen [1]. Evaluation of the elastic coefficients from RUS measurements is an inverse problem, i.e. the results are compared with computed eigenfrequencies of the specimen for successively precised guesses of the elastic coefficients. The inverse procedure for determination of the optimal elastic coefficients has been developed for rectangular specimens of isotropic materials, as well as for materials of cubic and orthotropic symmetry, with the principal axes of the material parallel to the specimen's edges [2].

However, the developed procedures are not sufficient for simultaneous determination of the elastic properties of both austenitic and martensitic phases of shape memory alloys. When a rectangular austenitic specimen is transformed into a single variant of martensite its shape changes into a general parallelepiped with general orientation of the orthotropic martensitic structure [3]. Vice-versa, if a martensitic specimen has a rectangular shape and basic orientation, it becomes nonrectangular and generally oriented when it returns to austenite. On this purpose, the procedure must be generalized for an arbitrary oriented parallelepiped. Another improvement of the technique is necessary due to the high anisotropy of the investigated materials. For such strongly anisotropic materials (anisotropy factor larger than 10 in the austenitic phase), the number of measured eigenfrequencies necessary for reliable inversion is significantly larger than for classical materials. For example, to obtain all elastic coefficients of an martensitic single crystal of CuAlNi, 120 frequencies were measured. For such extensive sets of the input data, a crucial point is to associate correctly the frequencies to modes of vibration, i.e. to compare, within the inverse procedure, physically corresponding frequencies. For this reason, the specimens were, during the measurements, scanned by a laser interferometer to obtain information about the shapes of particular eigenmodes. This method was firstly introduced by Ogi et al. in [4]. Involving the eigenmodes in the optimization process significantly stabilizes the whole procedure.

II. FREE ELASTIC VIBRATIONS OF AN ANISOTROPIC PARALLELELPIPED

Let us consider an anisotropic, nonrectangular parallelepiped in Fig.1. In the Cartesian coordinate system $\mathbf{x} = [\boldsymbol{x_1}, \boldsymbol{x_2}, \boldsymbol{x_3}]$, let the anisotropic elasticity be described by the tensor C_{ijkl} and the parallelepiped's faces have unit normals $\boldsymbol{n_1}$, $\boldsymbol{n_2}$, and $\boldsymbol{n_3}$.

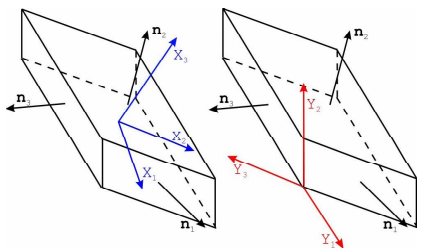

Figure 1. Geometry of the parallelepiped and introduction of Cartesian systems **x** and **y**.

An oblique coordinate system can be introduced by setting the axes $\mathbf{y} = [\boldsymbol{y_1}, \boldsymbol{y_2}, \boldsymbol{y_3}]$, parallel to the parallelepiped's edges.

Supported from the Marie-Curie Research Training Network MULTIMAT (MRTN-CT-2004-505226) and project no. 01/06/0768 of CSF.

For the origins of the systems **x** and **y** coinciding, their coordinates are related by linear equation

$$\boldsymbol{y} = \mathbf{B}\boldsymbol{x}\,, \tag{1}$$

where **B** is a nonsingular matrix given by:

$$\mathbf{B} = \begin{pmatrix} (\boldsymbol{n}_1)_{x_1} & (\boldsymbol{n}_1)_{x_2} & (\boldsymbol{n}_1)_{x_3} \\ (\boldsymbol{n}_2)_{x_1} & (\boldsymbol{n}_2)_{x_2} & (\boldsymbol{n}_2)_{x_3} \\ (\boldsymbol{n}_3)_{x_1} & (\boldsymbol{n}_3)_{x_2} & (\boldsymbol{n}_3)_{x_3} \end{pmatrix}. \tag{2}$$

The resonance frequencies and eigenvectors of such specimen can be sought by finding stationary points of the Lagrangian Λ

$$\Lambda = \frac{1}{2}\int_V \left[\rho\omega^2 u_i^2(\boldsymbol{x}) - C_{ijkl}\frac{\partial u_i}{\partial x_j}(\boldsymbol{x})\frac{\partial u_k}{\partial x_l}(\boldsymbol{x})\right]\mathrm{dV}\,, \tag{3}$$

where V is the specimen's volume, $\boldsymbol{u}(\mathbf{x})$ is the displacement field, ρ is the mass density, and ω is the sought eigenfrequency. The integration is performed over the whole volume, i.e. in the range

$$y_i \in \langle -d_i/2; +d_i/2\rangle, \qquad i = 1,2,3, \tag{4}$$

where d_i are the distances of corresponding parallel faces. Applying the substitution (**x**) → (**y**) given by (1) in the Lagrangian (3), we obtain

$$\Lambda = \frac{1}{2}\int_{-\frac{d_1}{2}}^{+\frac{d_1}{2}}\int_{-\frac{d_2}{2}}^{+\frac{d_2}{2}}\int_{-\frac{d_3}{2}}^{+\frac{d_3}{2}}\left[\frac{\rho}{\Im}\omega^2 u_i^2(y) - T_{ijkl}\frac{\partial u_i}{\partial y_j}(y)\frac{\partial u_k}{\partial y_l}(y)\right]\mathrm{d}y_1\mathrm{d}y_2\mathrm{d}y_3\,, \tag{5}$$

where $\Im = \det\mathbf{B}$ is the Jacobian of the considered transformation, and

$$T_{ijkl} = \frac{1}{\Im}C_{ipko}B_{jp}B_{lo}\,. \tag{6}$$

The four-dimensional array T_{ijkl} is does not have properties of a 4th order tensor, but it remains symmetric with respect to index doubles *ij* and *kl*. The advantage of using T_{ijkl} rather than a fully rotated tensor lies in considerably faster evaluation of this array. Moreover, this approach keeps the displacement vectors **u** in the original coordinate system **x** (even if they are function of oblique coordinates **y**,) which simplifies final evaluation of the eigenmodes. For Lagrangian (5), the Ritz method can be applied by taking base functions in the form

$$\Psi_{abc} = P_a\left(\frac{2y_1}{d_1}\right)P_b\left(\frac{2y_2}{d_2}\right)P_c\left(\frac{2y_3}{d_3}\right)$$
$$a, b, c = 0,1,2,3\ldots \qquad a+b+c \le N\,, \tag{7}$$

where $P_n(y)$ is the Legendre polynomial of degree n defined as

$$P_n(y) = \frac{1}{2^n n!}\left[\frac{d^n}{dx^n}(x^2-1)^n\right]. \tag{8}$$

Searching for stationary points of the Lagrangian Λ leads to a symmetric eigenvalue problem

$$\left(\omega^2\mathbf{E}_{[abc,i],[def,j]} - \mathbf{\Gamma}_{[abc,i],[def,j]}\right)\alpha_{[abc,i]} = 0\,, \tag{9}$$

where

$$\mathrm{E}_{[abc,i],[def,j]} = \delta_{ij}\delta_{ad}\delta_{be}\delta_{cf}\,, \tag{10}$$

$$\mathbf{\Gamma}_{[abc,i],[def,j]} = \frac{\Im}{\rho}\frac{8}{d_1d_2d_3}T_{ijkl}\int_{-\frac{d_1}{2}}^{+\frac{d_1}{2}}\int_{-\frac{d_2}{2}}^{+\frac{d_2}{2}}\int_{-\frac{d_3}{2}}^{+\frac{d_3}{2}}\frac{\partial\Psi_{abc}}{\partial y_k}\frac{\partial\Psi_{def}}{\partial y_l}\mathrm{d}y_1\mathrm{d}y_2\mathrm{d}y_3 \tag{11}$$

and $\alpha_{[abc,i]}$ are coefficients of the eigenvector in the basic functions given above. The Cholesky algorithm, implemented in the standard Matlab routine **`eig.m`**, was used for determination of both the eigenfrequencies and eigenvectors of (9).

III. INVERSION PROCEDURE

To evaluate the elastic constants, one must first solve the forward problem of calculating the natural frequencies from the elastic constants, and apply a nonlinear inversion procedure to find the required elastic constants from the measured natural frequencies. It represents nonlinear minimization in the sense of the least square method of the objective function

$$F(C_{ijkl}) = \sum_p\left(\frac{\omega_{p\,cal}^2(C_{ijkl}) - \omega_{p\,\exp}^2}{\omega_{p\,\exp}^2}\right)^2, \tag{12}$$

where $\omega_p^2{}_{cal}$ and $\omega_p^2{}_{exp}$ are associated calculated and measured eigenvalues of p^{th} measured mode. Reliable mode association is crucial for stability of the inversion and can be achieved by displacement field measurement on the vibrated specimen using scanning laser interferometry described below.

The accuracy of the calculated frequencies requires using a high degree N of the Legendre polynomials. On the other hand, the order of the symmetric matrix $\mathbf{\Gamma}$ increases rapidly with increasing N (e.g. for N = 16 is 2907), which also rapidly increases computation time. A useful reduction of the number of forward calculation can be done deriving gradient and Hessian of the objective function. Choosing the eigenvectors α_j of the matrix $\mathbf{\Gamma}$ to form orthogonal normalized system, and using the linear dependency of the coefficients of matrix $\mathbf{\Gamma}$ on C_{ijkl}, we obtain from the theory of perturbation:

$$\frac{\partial\omega_j^2}{\partial C_k} = \alpha_j^T\frac{\partial\Gamma}{\partial C_k}\alpha_j \tag{13}$$

$$\frac{\partial^2\omega_j^2}{\partial C_k\partial C_l} = \alpha_j^T\frac{\partial\Gamma}{\partial C_k}\frac{\partial\alpha_j}{\partial C_l} + \left(\frac{\partial\alpha_j}{\partial C_l}\right)^T\frac{\partial\Gamma}{\partial C_k}\alpha_j\,, \tag{14}$$

where

$$\frac{\partial\alpha_j}{\partial C_l} = \sum_{\substack{i \\ \omega_i\neq\omega_j}}\frac{\alpha_i^T\frac{\partial\Gamma}{\partial C_l}\alpha_j}{\omega_j^2-\omega_i^2}\alpha_i\,, \tag{15}$$

with C_k denoting the set of independent elastic constants for given material symmetry. The matrixes $\partial\Gamma/\partial C_k$ are independent

on elastic constants C_k and can be evaluated previously. More, completion of the matrix Γ can be simply done considering

$$\Gamma = (\partial\Gamma/\partial C_k)\, C_k \,. \qquad (16)$$

A novel hybrid architecture of the inverse problem solution, combining both gradient and simplex method, was developed to solve this optimizing problem. In every step of the simplex method, the gradient Levenberg-Marquardt algorithm is released from a starting point given by the actual position of the simplex. In the other words, the simplex method is optimizing the starting points for the Levenberg-Marquardt method. Such complex algorithm combines the robustness of a simplex search with an efficiency of the gradient method.

IV. Experimental Setup

The experimental setup for RUS experiments is outlined in Fig.2. It consists of a National Instruments PXI high speed digital I/O system including a waveform generator and a two-channels digitizer which enables synchronized sampling of both output and input cards. The broadband chirp signal is generated by the high frequency D/A converter and, after the amplification, excites the specimen by miniature piezoelectric transducer placed on the specimen's corner. The displacement response is detected in a mesh of points on the sample surface by means of the laser interferometer (Polytec OFV-2570) equipped with an original scanning unit consisting of two dielectric mirrors on motorized positional stages. The unit is used for equidistant scanning of the specimen's surface with precision up to 1.25μm. The frequency responses in individual points of the mesh are acquired automatically.

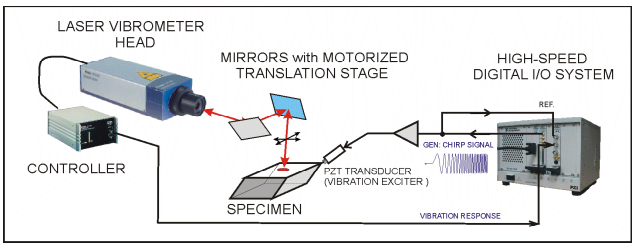

Figure 2. Experimental setup.

Besides the mode identification mentioned in the introduction, another advantage of such point to point noninvasive measurement of vibrational sample response is that we avoid omitting of some resonances at signal detection near node points (zero-valued points of vibrational modes) by averaging the magnitudes of measured spectra over different points on the sample surface. Examples of measured and computed eigenmodes of a martensitic parallelepiped of a CuAlNi shape memory alloy are shown in Fig.3. The examined was a nonrectangular 3.6mm × 4.2mm × 4.0mm parallelepiped with face normals orientation close to [010] [-1 0 1] [1 0 1].

V. Applications of Proposed Methods

The above described method was applied to determine all elastic coefficients of pure phases of the CuAlNi shape memory alloys. The temperature dependence of these coefficients at temperatures close to the phase transition temperature illustrates shear softening of the material prior to the transitions. Examples of the investigated thermal dependences are shown in Fig.4, where the behaviors of corresponding elastic parameters of both phases are compared. The coefficients C_{MS} and C_S (introduced by authors in [3]) are the combinations of elastic constants corresponding to minimal shear velocities in particular phases, A^{ort} and A are the anisotropy coefficients.

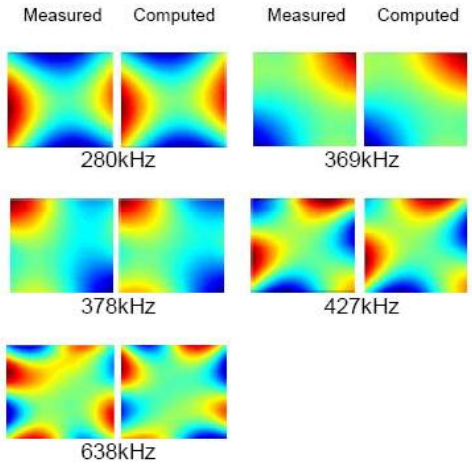

Figure 3. Example of comparison of measured and computed shapes of eigenmodes of a CuAlNi martensitic specimen.

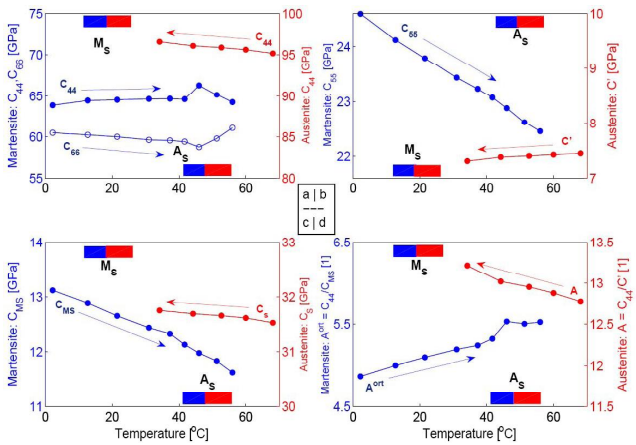

Figure 4. Thermal dependences of elastic properties of the CuAlNi shape memory alloy in vicinity of phase transitions.

Applicability of the proposed method for a general parallelepiped enabled this method to be also used for determination of effective elastic properties of finely twinned martensitic structures. As a testing material, the CuAlNi alloy was chosen again. However, the main possible income of such measurements lies in experimental investigation of naturally twinned materials, such as NiMnGa, where the single crystals of pure martensitic variants cannot be easily prepared.

TABLE I. MEASURED AND EVALUATED EFFECTIVE ELASTIC COEFFICIENS OF FINELY TWINNED MARTENSITE OF CUALNI

Elastic Coefficient	Relative contents of the mirrored variant [%]		
	< 1%	*~ 10%*	*10% evaluated*
C_{11} [GPa]	185.3	191.2	189.7
C_{22} [GPa]	151.3	150.5	150.7
C_{33} [GPa]	241.9	236.4	236.0
C_{44} [GPa]	63.2	64.2	63.5
C_{55} [GPa]	23.9	24.1	25.5
C_{66} [GPa]	62.0	62.0	61.1
C_{23} [GPa]	88.0	98.2	92.2
C_{13} [GPa]	67.8	64.9	65.3
C_{12} [GPa]	141.8	138.8	140.7

The result are shown in Tab.1, where the coefficients of the single variant (<1% of other variants) are compared to measured and evaluated elastic coefficients for finely twinned martensite, containing approximately 10% of a mirrored variant. The coefficients of a single variant are in good agreement with the results from pulse-echo measurements published by authors in [3]. The theoretical effective coefficients of the twinned structure were computed by an algorithm based on the Snell-Descartes law. Especially in the diagonal coefficients C_{11}, C_{22} and C_{33}, the agreement between measured and evaluated elastic coefficients is satisfactory. However, the symmetry of the twinned structure deviates from orthotropy, which may be the reason for the discrepancy in determined shear coefficients.

VI. CONCLUDING REMARKS

The inversion procedure for determination of elastic coefficients of anisotropic solids was generalized for an arbitrary oriented nonrectangular parallelepiped. The procedure was also stabilized by using a novel hybrid architecture of the optimizing algorithm, which utilizes analytical expressions of the Hessian of the minimized error function. Laser interferometry was used for association of measured frequencies to particular eigenmodes. The agreement between measured and computed shapes of the eigenmodes confirms the reliability of obtained elastic coefficients.

The improved inversion procedure was applied to determine elastic coefficients of both the austenitic and martensitic phases of the CuAlNi shape memory alloy, as well as of effective elastic coefficient of twinned martensitic structures. The procedure was verified as stable, fast, and converging to reliable values of the elastic coefficients.

ACKNOWLEDGMENT

The authors would like to acknowledge Dr. J. Plešek for helpful comments on the presented theory.

REFERENCES

[1] W. M. Visscher, A. Migliori, T. M.Bell, and R.A. Reinert, "On the normal modes of free vibration of inhomogeneous and anisotropic elastic objects," J. Acoust. Soc. Am., vol. 90, pp. 2154–2162, October 1991.

[2] A. Migliori, J.L. Sarrao, W.M. Visscher, T.M. Bell, M. Lei, Z. Fisk, and R. G. Leisure, "Resonant ultrasound spectroscopic techniques for measurement of the elastic moduli of solids," Physica B, vol. 183, pp. 1–24, January 1993.

[3] P. Sedlák, H. Seiner, M. Landa, V. Novák, P. Šittner and Ll. Mañosa, "Elastic constants of bcc austenite and 2H orthorhombic martensite in CuAlNi shape memory alloy," Acta Materialia, vol. 53, Pages 3643-3661, August 2005.

[4] H. Ogi, K. Sato, T. Asada, and M. Hirao, "Complete mode identification for resonance ultrasound spectroscopy." J Acoust. Soc. Am, vol. 112, pp. 2553-2557, December 2002.